The effect of improved chromatography on GDGT based paleoproxies

Ellen C. Hopmans[1,*], Stefan Schouten[1,2], Jaap S. Sinninghe Damsté[1,2]

[1]*NIOZ Royal Netherlands Institute for Sea Research, Department of Marine Organic Biogeochemistry, P.O. Box 59, 1790 AB Den Burg (Texel), The Netherlands*

[2] *Utrecht University, Faculty of Geosciences, Budapestlaan 4, 3584 CD Utrecht, The Netherlands*

[*]Corresponding author: ellen.hopmans@nioz.nl

Resubmitted to: *Organic Geochemistry*

Keywords: HPLC, GDGTs, TEX_{86}, MBT, CBT, proxies

Abstract

The development of methods using liquid chromatography coupled to mass spectrometry to analyze glycerol dialkyl glycerol tetraethers (GDGTs) has substantially expanded the biomarker tool box and led to the development of several new proxies. Recent studies have shown that new high performance liquid chromatography methods have substantially improved separation of GDGT isomers and detection of novel isomers. Here we present a chromatographic method based on 2 ultra high performance liquid chromatography silica columns capable of separating a wide range of GDGTs with good resolution and which compares favorably with previously published methods. This method was tested on a part of the global calibration set of the TEX_{86}, a proxy for sea water temperature, and on a part of the global calibration set of the MBT_{5Me}, a proxy for air temperature, and CBT', a proxy for soil pH. Our results show that the new high resolution chromatography method leads to a significant but small offset (<0.01 or <0.8 °C) in TEX_{86}, especially at low values, while no difference is observed for the CBT'. However, for the MBT_{5Me} a significant difference is observed (<0.01 or <3 °C), especially at low values, although this difference is smaller than the calibration error (4.8 °C).

1. Introduction

Over the past decade, research into the environmental occurrence and geochemical importance of glycerol dialkyl glycerol tetraethers (GDGTs) has expanded enormously. The development of high performance liquid chromatography (HPLC)–mass spectrometry (MS) methodology (Hopmans et al., 2000) allowed analysis of the core lipids, instead of more laborious GC-MS analysis of the released carbon chains after ether cleavage. This led to the discovery of a range of new GDGTs, including crenarchaeol (Sinninghe Damsté et al., 2002) produced by Thaumarchaeota, and GDGTs with branched carbon skeletons (brGDGTs), most likely produced by soil bacteria (Sinninghe Damsté et al., 2000). These novel GDGTs were found to be widespread in

marine and terrestrial environments (Schouten et al., 2000 and 2013a) and several new geochemical proxies have since been introduced based on their distributions.

Schouten et al. (2002) introduced the TEX_{86} for reconstruction of sea surface temperatures based on GDGTs produced by marine Thaumarchaeota, comprising GDGTs 1-3 (numbers indicate the number of cyclopentane moieties) and the regioisomer of crenarchaeol. Hopmans et al. (2004) defined the BIT index, quantifying the relative abundance of the branched GDGTs versus crenarcharchaeol, to estimate the input of terrestrial organic matter into marine sediments. The relative distribution of branched GDGTs in soils was shown by Weijers et al. (2007) to contain information on mean annual air temperature and soil pH, which led to the definition of the CBT and MBT indices, respectively. Proxies based on GDGTs are now increasingly used in palaeoclimatology, palaeoceanography and palaeolimnology to reconstruct palaeoenvironmental parameters (e.g. Schouten et al., 2013a; Pearson and Ingalls, 2013).

Currently, the most commonly used analytical methodology (Schouten et al., 2013b) is a normal phase separation on a cyano (CN) column using mixtures of hexane and isopropanol as mobile phase followed by positive ion atmospheric pressure chemical ionization (APCI)-MS detection in selected ion monitoring (SIM) mode of the protonated molecules of the various GDGTs (Schouten et al., 2007). A complication in the accurate quantification of the GDGTs used in the various proxies is the imperfect separation of the various isomers of the GDGTs, resulting in both earlier eluting (as frequently observed for the isoprenoid GDGTs) or later eluting shoulders (in case of the branched GDGTs). The standard integration protocol (Schouten et al., 2009) calls for exclusion of these shoulders during integration, however, the accuracy with which this can be achieved is dependent on the quality of the chromatography, the complexity of the GDGT distribution, and the relative abundance of the isomers, resulting in analytical uncertainties.

Recently, De Jonge et al. (2013) identified the components responsible for the late eluting shoulder often observed on the chromatographic peaks of branched GDGTs. These were found to comprise 6-methyl brGDGT rather than the 5-methyl brGDGTs. Subsequently, De Jonge et al. (2014)

showed that improved HPLC separation, allowing more precise and separate quantification of the various isomers of the branched GDGTS, greatly impacted the CBT and MBT paleoproxies. The newly defined MBT'$_{5Me}$, which excludes the 6-methyl brGDGT, is no longer related to soil pH and showed an improved correlation with mean annual air temperature (MAT), while the newly defined CBT', now including the 6-methyl brGDGTs, showed a much improved pH reconstruction. This improved separation was achieved by 4 HPLC silica columns in series but resulted in a total run time of 4 h, three times as long as the commonly used method. Recently, several improvements in chromatography for GDGTs were reported. Zech et al. (2012) reported improved separation between the hexamethylated brGDGTS, while Becker et al. (2013) reported improved chromatography for isoprenoid GDGTs using 2 Ultra (U)HPLC BEH amide columns in tandem. In addition, Yang et al. (2015) reported improved separation of brGDGTs using 2 UHPLC silica columns in tandem.

Here we present a chromatographic method using 2 UHPLC silica columns in series, that leads to baseline separation of the various isomers of the branched GDGTs, and which is fully compatible with most standard LC systems. A total analysis time of 90 minutes affords analysis of all GDGTs used for calculating TEX_{86}, CBT, and MBT, as well as hydroxyl (OH-) and dihydroxyl (2-OH-) GDGTs and other more recently described GDGTs (e.g. Liu et al, 2012a and 2012b). We compared our method with previously published ones and tested the impact of improved chromatography on GDGT-based proxies by analyzing a subset of samples used in the global TEX_{86} calibration by Kim et al. (2010) and the global CBT/MBT calibration by De Jonge et al. (2014).

2. Material and Methods

2.1 *Samples*

A representative subset of 26 samples, with TEX_{86} values ranging from 0.36 to 0.71, was selected from the samples previously used for the TEX_{86} calibrations by Kim et al. (2010) for re-analysis on the UHPLC columns as described below. These samples were also re-analyzed with the

same LC-MS instrument using the traditional method according to Schouten et al. (2007) to prevent instrument bias impacting on the comparison of the TEX_{86} values. For comparison of MBT and CBT indices, a selection of 36 samples, previously analyzed with 4 Si columns in series by De Jonge et al. (2014), was made. These samples had MBT values ranging from 0.25 to 0.99, and CBT values ranging from -0.05 to 2.59. In addition, 2 composite samples (D1 and D2) from a piston core from Drammensfjord (Norway; D2-H; 59 40.11 N, 10 23.76 E; water depth 113 m) were used to evaluate the effects of improved chromatography on the BIT index. One of these (D1) is identical to interlaboratory standard S1 in the 2009 TEX_{86} and BIT interlaboratory study (Schouten et al., 2009). To prevent instrument bias, these samples were reanalyzed using both the new method and according to Schouten et al. (2007) on the instrument described below.

2.2 *UHPLC-MS GDGT analysis*

Analysis was performed on an Agilent 1260 UHPLC coupled to a 6130 quadrupole MSD in selected ion monitoring mode. Separation was achieved on two UHPLC silica columns (BEH HILIC columns, 2.1 x 150 mm, 1.7 μm; Waters) in series, fitted with a 2.1 x 5 mm pre-column of the same material (Waters) and maintained at 30˚C. GDGTs were eluted isocratically for 25 min with 18% B, followed by a linear gradient to 35% B in 25 min, then a linear gradient to 100% B in 30 min, where A is hexane and B is hexane: isopropanol (9:1). Flow rate was 0.2 ml/min, resulting in a maximum back pressure of 230 bar for this chromatographic system. Total run time is 90 min with a 20 min re-equilibration. Source settings were identical to Schouten et al. (2007). Typical injection volume was 5 μl of a 2mg/ml solution of polar fractions obtained after aluminum oxide chromatography (Schouten et al., 2009).

In selected cases, samples were analyzed by UHPLC-high resolution accurate mass MS (HRAM/MS) on a ThermoScientific UltiMate 3000 RS series UHPLC with thermostatted auto-injector and column compartment coupled to a ThermoScientific Q Exactive Orbitrap mass spectrometer using the same chromatographic method as described above. The positive ion APCI settings were as

follows; probe heater temperature, 350°C; sheath gas (N_2) pressure, 50 AU (arbitrary units); auxiliary gas (N_2) pressure, 5 AU; spray current, 5 µA; capillary temperature, 275°C; S-lens, 100 V. Target lipids were analyzed with a mass range of *m/z* 900 to 1500 (resolution, 70000), followed by data dependent MS^2 (resolution, 17500), in which the five most abundant masses in the mass spectrum were fragmented (stepped normalized collision energy 15, 20, 25; isolation width 1.0 Da). The Q Exactive was calibrated within a mass accuracy range of 1 ppm using the Pierce LTQ Velos ESI Positive Ion Calibration Solution (containing a mixture of caffeine, MRFA, Ultramark 1621, and *N*-butylamine in an acetonitrile-methanol-acetic solution; Thermo Scientific).

TEX_{86} values were calculated as defined by Schouten et al. (2002) and the BIT index according to Hopmans et al. (2004). Peak areas of the 5- and 6-methyl isomers of the branched GDGTs were combined for calculation of the BIT index. MBT'_{5Me}, CBT_{5Me} and CBT' were calculated according to De Jonge et al. (2014).

The ***c***hromatographic resolution for various critical pairs was calculated using the following equation (Snyder et al, 1997):

$$Rs = 1.18(t_2-t_1)/(W_{0.5,1} + W_{0.5,2}) \quad [1]$$

where t_1 and t_2 are the retention times of the critical pair peak, and $W_{0.5}$ refers to peak width at half peak height.

For all calculated indices, differences in the index values between methods were assessed with paired t-tests. Differences were considered significant if $P<0.05$.

3. Results and Discussion

3.1 Chromatography

The improved chromatography due to the use of 2 UHPLC silica columns in series is illustrated in Fig. 1 for composite sediment D2 from Drammensfjord, Norway. The resolution between several critical pairs of GDGTs is shown in table 1. The base peak chromatogram (Fig. 1A)

131 shows the isoprenoid GDGTs eluting from 15 to 30 minutes, the brGDGTs eluting from 40 to 55 min,
132 while OH-GDGTs (Liu et al., 2012b) and di-OH-GDGTs (not visible in the chromatogram shown in Fig.
133 1 due to low abundance) elute between 68 to 73 min and 82 to 87 min, respectively. Analysis of this
134 extract using the same chromatographic setup but using a high resolution/accurate mass MS
135 revealed that other previously reported ether lipids such as so called "sparsely and overly" branched
136 GDGTs (e.g. Liu et al, 2012a), glycerol monoalkyl glycerol tetraethers or "H-shaped' GDGTs (e.g.
137 Schouten et al., 2008), glycerol dialkanol diethers (Knappy and Keely, 2012; Liu et al, 2012c) eluted
138 within the analytical window shown and in the same relative retention order as previously reported.
139 The C_{46} glycerol trialkyl glycerol tetraether internal standard (cf. Huguet et al., 2006), elutes at 30 min
140 and is separated from the regioisomer of crenarchaeol (cren') with which it typically co-elutes on the
141 CN column.
142 The dominant isomers of GDGT-1, -2, and -3, used in the TEX_{86}, are now clearly separated
143 from the previously partially co-eluting minor isomers (Fig. 1B). In fact, often multiple isomers of
144 each GDGT are revealed, sometimes with larger apparent abundance than the isomers used in the
145 TEX_{86}. The exact structure of these isomers is unknown, but likely are varying stereoisomers,
146 parallel/anti-parallel conformations and/or GDGTs with unsaturations (Zhu et al.,2014).
147 Crenarchaeol (cren) and its regioisomer (cren') are fully separated from each other (Fig. 1D).
148 However, in many samples a third isomer of crenarchaeol eluting between crenarchaeol and its
149 regioisomer is also observed. GDGT-4 elutes as a well-defined shoulder in front of crenarchaeol, with
150 a resolution between peaks of 1.07 (data not shown). Comparison of the resolutions achieved with
151 the standard CN method, the method of Becker et al. (2013) and our new method (Table 1) shows
152 that the highest resolutions are achieved using our 2 UHPLC silica column method for all critical pairs
153 of the isoprenoid GDGTs.
154 Separation achieved for the brGDGTs on 2 UHPLC silica columns (Fig. 1B) is almost identical
155 to the improved separation on four HPLC silica columns as reported by De Jonge et al (2014), but
156 with further improved resolution (Table 1). The 5- and 6-methyl-hexamethylated brGDGTs are

baseline separated (Rs>1.5). Close examination of the chromatograms often reveals a small peak eluting between the 5- and 6-methyl-hexamethylated brGDGTs (Fig IE). This peak represents the 5/6-methyl-hexamethylated brGDGT, recently identified by Weber et al. (2015). Baseline separation is not achieved for the pentamethylated brGDGTs, although the separation is also slightly improved over the 4 x HPLC silica method (Table 1). Becker et al. (2013) did not achieve baseline separation between 5- and 6-methyl-hexamethylated brGDGTs using 2 UHPLC BEH amide columns, although resolutions were not reported for these critical pairs. Yang et al. (2015) reported an improved separation of brGDGTs very similar to the separation presented here, also using 2 UHPLC silica columns in tandem but with an alternative solvent system of hexane/ethyl acetate. Unfortunately, they did not report the resolution of the various critical pairs of brGDGTs, making a quantitative comparison between the methods difficult.

Further improvements in separation can be expected by the addition of more UHPLC columns. Several GDGT peaks show hints of shoulders, and peak width varies more than expected for chemically similar compounds. However, this would result in a substantial increase in analysis time, which is undesirable for a routine method used to generation high resolution paleoclimate records.

3.2 Effect of the new separation system on GDGT proxies

In order to assess the impact of the improved separation achieved on the UHPLC columns, we reanalyzed a subset of samples, previously analyzed for the global calibration sets of Kim et al. (2010) for the TEX_{86}, and De Jonge et al. (2014) for the CBT/MBT. The samples were chosen to cover the broadest index ranges possible. We reanalyzed the selected samples for TEX_{86} on the same HPLC-MS as used for the UHPLC columns, but using the CN column to avoid differences resulting from the use of a different HPLC-MS system. All values are listed in the Supplementary Information.

3.2.1 TEX_{86}

183 A cross plot of the values for $TEX_{86, UHPLC}$ vs. the $TEX_{86, CN}$ shows that the UHPLC method
184 returns slightly lower TEX_{86} values (P= 0.001) compared to the CN column, with larger deviations for
185 TEX_{86} values in the lower range (Fig. 2A). This is likely caused by a reduction of peak area due to
186 removal of co-eluting peaks, which will result in lower integrated peak areas, especially in samples
187 with an already low TEX_{86} and low relative abundances of GDGTs 1-3. However, it should be noted
188 that the differences between the two methods is very small with an average of 0.005 TEX_{86} unit and
189 even for samples in the lower range this typically does not exceed 0.01 unit, representing a 0.8 ˚C
190 deviation, which is well within the reported calibration error of 2.5 ˚C reported by Kim et al. (2010)
191 as well as interlaboratory differences which range between 1.3 to 3.0 ˚C (Schouten et al., 2013b).
192
193 *3.2.2. MBT'$_{5Me}$ index*
194 The effect of the improved UHPLC separation on mean annual air temperature (MAT)
195 reconstructions was assessed by comparing MBT'$_{5Me}$ values to those determined on the 4 x Si
196 method. A comparison with the CN column method is in this case impossible as the 5- and 6-methyl-
197 brGDGTS are not well separated using this method. The MBT'$_{5Me, UHPLC}$ is systematically lower
198 (P<<0.001) compared to the 4xSi MBT'$_{5Me, 4xSi}$ and the offset increases with lower MBT'$_{5Me}$ values
199 (Figure 2B). This is most likely due to the increased sensitivity of the new separation method to
200 detect the hexamethylated brGDGTs, and pentamethylated brGDGTs with cyclopentane moieties,
201 which are notoriously hard to detect, especially in samples from colder regions (De Jonge et al.,
202 2014). Improved peak shape (decreased peak width and increased peak height) due to the use of
203 UHPLC columns will, in some cases, lead to the detection of these previously non-detectable GDGTs.
204 As the hexa- and pentamethylated brGDGTs with cyclopentane rings are only represented in the
205 denominator of the MBT'$_{5Me}$ equation, this will lead to lower MBT'$_{5Me}$ values and lower
206 reconstructed MAT temperatures. Interestingly, De Jonge et al. (2014) shows a systematic
207 overestimation of the MAT reconstruction vs. the measured MAT in soils from colder regions where
208 penta- and tetramethylated brGDGTs are often below the detection limit, which may partially be

corrected by the improved chromatography. It should be noted that even for samples in the lower MBT'$_{5Me}$ range, the offset does not exceed 0.01 unit, representing a ~3 ˚C deviation, which is still within the reported calibration error of 4.8 ˚C (De Jonge et al., 2014).

3.2.3 CBT$_{5Me}$ and CBT' indices

Comparison of the CBT$_{5Me}$ and CBT' values generated using the 2 UHPLC column versus the values obtained with 4 x Si columns shows that CBT$_{5Me,4xSi}$ values are slightly but significantly lower ($P = 0.04$) than the CBT$_{5Me, uhplc}$ values with an average difference of 0.02 units. This difference is largely driven by one outlier and is reduced to 0.008 when this value is removed. Furthermore, a difference of 0.02 CBT$_{5Me}$ unit represents a change in reconstructed pH of 0.03 which is well below the reported calibration error of 0.84 (De Jonge et al, 2014). CBT'$_{uhplc}$ values are not significantly different from CBT'$_{4xSi}$ values, with an average difference of 0.008, representing 0.01 pH unit.

3.2.4 BIT index

The BIT index of the samples discussed above were all either very low (marine, <0.05) or very high (soils, >0.95) making comparisons of chromatography methods difficult. Therefore, the impact of the improved chromatography on the BIT index was assessed using composite sediment samples D1 and D2 from Drammersfjord, Norway which have intermediate BIT values. The BIT$_{UHPLC}$ is consistently higher than the BIT$_{CN}$ for both samples. BIT$_{CN}$ and BIT$_{UHPLC}$ for sample D1 were 0.59 ± 0.01 (n=3) vs. 0.63 ± 0.01 (n=5) and 0.75 ± 0.01 (n=5) vs. 0.78 ± 0.01 (n=5) for sample D2. However, it should be noted that the BIT index is a qualitative measure for soil organic matter input into marine sediments and round robin studies (Schouten et al, 2009 and 2013) showed interlaboratory differences for the BIT index much larger than observed here, making the small shift in values due to improved chromatography inconsequential.

4. Conclusions

Here we have described improved chromatography for GDGTs using 2 UHPLC silica columns with improved resolution of all critical GDGT pairs compared to previously reported chromatographic methods. The improved chromatography has no effect on the CBT', while the differences observed for the TEX_{86} and the CBT_{5Me} fall well within the reported error for the current global calibrations. A significant change in obtained values for the BIT index was observed, but as this index is qualitative only, the use of this index to inventory relative changes in soil organic matter input into marine sediments is not affected. Re-calibration of the MBT_{5Me} could be warranted as a significant off set is observed from values determined on 4 x Si columns, especially for samples from cold regions. The improved resolution, improved sensitivity due to reduced peak widths and resulting enhanced peak heights (sample use is half from the traditional method), coupled to an acceptable analysis time should allow the generation of high resolution climate records while having improved indices.

Acknowledgements

We would like to thank Dr. Cindy de Jonge, Jung-Hyun Kim, and Francien Peterse for providing sample material. We would also like to thank Dr. Julius Lipp and an anonymous reviewer for reviewing this manuscript. This work was carried out under the program of the Netherlands Earth System Science Centre (NESSC), financially supported by the Ministry of Education, Culture and Science (OCW).

References

Becker, K.W., Lipp J.S., Zhu, C., Liu X-L., Hinrichs, K.U. , 2013. An improved method for the analysis of archaeal and bacterial ether core lipids. Organic Geochemistry 61, 34–44.

De Jonge, C., Hopmans, E. C., Stadnitskaia, A., Rijpstra, W. I. C., Hofland, R., Tegelaar, E., Sinninghe Damsté, J. S., 2013. Identification of novel penta- and hexamethylated branched glycerol dialkyl glycerol tetraethers in peat using HPLC-MS^2, GC-MS and GC-SMB-MS. Organic Geochemistry 54, 78–82.

De Jonge, C., Hopmans, E.C., Schouten, S., Sinninghe Damsté, J.S., 2014. Occurrence and abundance of 6-methyl branched glycerol dialkyl glycerol tetraethers in soils: Implications for palaeoclimate reconstruction. Geochim. Cosmochim. Acta 141, 97-112.

Hopmans, E.C., Schouten, S., Pancost, R.D., van der Meer, M.T.J., Sinninghe Damsté, J.S., 2000. Analysis of intact tetraether lipids in archaeal cell material and sediments by high performance liquid chromatography/atmospheric pressure chemical ionization mass spectrometry. Rapid Communications in Mass Spectrometry 14, 585–589.

Hopmans, E.C., Weijers, J.W.H., Schefuss, E., Herfort, L., Sinninghe Damsté, J.S., Schouten, S., 2004. A novel proxy for terrestrial organic matter in sediments based on branched and isoprenoid tetraether lipids. Earth and Planetary Science Letters 24, 107–116.

Huguet, C., Hopmans, E.C., Febo-Ayala, W., Thompson, D.H., Sinninghe Damsté, J.S., Schouten, S., 2006. An improved method to determine the absolute abundance of glycerol dibiphytanyl glycerol tetraether lipids. Organic Geochemistry 37, 1036-1041.

Kim, J.-H., van der Meer, J., Schouten, S., Helmke, P., Willmott, V., Sangiorgi, F., Koç, N., Hopmans, E.C., Sinninghe Damsté. J.S., 2010. New indices and calibrations derived from the distribution of crenarchaeal isoprenoid tetraether lipids: Implications for past sea surface temperature reconstructions. Geochimica et Cosmochimica Acta 74, 4639-4654.

Knappy, C.S., Keely, B.J., 2012. Novel glycerol dialkanol triols in sediments: transformation products of glycerol dibiphytanyl glycerol tetraether lipids or biosynthetic intermediates? Chemical Communications 48, 841-843.

Liu, X-L., Summons R.E., Hinrichs, K.U., 2012a. Extending the known range of glycerol ether lipids in the environment: structural assignments based on tandem mass spectral fragmentation patterns. Rapid Communications in Mass Spectrometry 26, 2295-2302.

Liu, X.L., Lipp, J.S., Simpson, J.H., Lin Y.S., Summons, R.E., Hinrichs, K.-U., 2012b. Mono- and dihydroxyl glycerol dibiphytanyl glycerol tetraethers in marine sediments: Identification of both core and intact polar lipid forms. Geochimica et Cosmochimica Acta 89, 102-115.

287 Liu, X.L., Lipp, J.S., Schröder, J.M., Summons, R.E., Hinrichs, K.U., 2012c. Isoprenoidal glycerol dialkanol
288 diethers: a series of novel archaeal lipids in marine sediments. Organic Geochemistry 43, 50-55.
289 Pearson, A., Ingalls, A. E., 2013. Assessing the use of archaeal lipids as marine environmental proxies.
290 Annual Review of Earth and Planetary Sciences 41, 15.1–15.26.
291 Schouten, S., Hopmans E.C., Pancost R.D., and Sinninghe Damsté J.S., 2000. Widespread occurrence of
292 structurally diverse tetraether membrane lipids: Evidence for the ubiquitous presence of low-
293 temperature relatives of hyperthermophiles. Proceedings of the National Academy of Sciences
294 USA 97, 14421-14426.
295 Schouten, S., Hopmans, E.C., Schefuß, E., Sinninghe Damsté, J.S., 2002. Distributional variations in
296 marine crenarchaeotal membrane lipids: a new tool for reconstructing ancient sea water
297 temperatures? Earth and Planetary Science Letters 204, 265-274.
298 Schouten, S., Huguet, C., Hopmans, E.C., Sinninghe Damsté, J.S., 2007. Improved analytical
299 methodology of the TEX_{86} paleothermometry by high performance liquid
300 chromatography/atmospheric pressure chemical ionization-mass spectrometry. Analytical
301 Chemistry 79, 2940-2944.
302 Schouten, S., Baas, M., Hopmans, E.C., Sinninghe Damsté, J.S., 2008. An unusual isoprenoid tetraether
303 lipid in marine and lacustrine sediments. Organic Geochemistry 39, 1033-1038.
304 Schouten, S., Hopmans, E.C., van der Meer, J., Mets, A., Bard, E., Bianchi, T., Diefendorf, A., Escala, M.,
305 Freeman, K., Furukawa, Y., Huguet, C., Ingalls, A., Menot-Combes, G., Nederbragt, A., Oba, M.,
306 Pearson, A., Pearson, E., Rosell-Mele, A., Schaeffer, P., Shah, S., Shanahan, T., Smith, R.,
307 Smittenberg, R., Talbot, H., Uchida, M., Van Mooy, B., Yamamoto, M., Zhang, Z., Sinninghe
308 Damsté, J., 2009. An interlaboratory study of TEX_{86} and BIT analysis using high performance liquid
309 chromatography/mass spectrometry. Geochemistry, Geophysics, Geosystems 10, Q03012,
310 doi:10.1029/2008GC002221.
311 Schouten, S., Hopmans, E.C. and Sinninghe Damsté, J.S., 2013a. The organic geochemistry of glycerol
312 dialkyl glycerol tetraether lipids: a review. Organic Geochemistry 54, 19–61.

313 Schouten, S., Hopmans, E. C., Rosell-Melé, A., Pearson, A., Adam, P., Bauersachs, T., Bard, E.,
314 Bernasconi, S. M., Bianchi, T. S., Brocks, J. J., Carlson, L. T., Castañeda, I. S., Derenne, S., Selver,
315 A. D., Dutta, K., Eglinton, T., Fosse, C., Galy, V., Grice, K., Hinrichs, K.-U., Huang, Y., Huguet, A.,
316 Huguet, C., Hurley, S., Ingalls, A., Jia, G., Keely, B., Knappy, C., Kondo, M., Krishnan, S., Lincoln,
317 S., Lipp, J., Mangelsdorf, K., Martínez-García, A., Ménot, G., Mets, A., Mollenhauer, G., Ohkouchi,
318 N., Ossebaar, J., Pagani, M., Pancost, R. D., Pearson, E. J., Peterse, F., Reichart, G.-J., Schaeffer,
319 P., Schmitt, G., Schwark, L., Shah, S. R., Smith, R. W., Smittenberg, R. H., Summons, R. E., Takano,
320 Y., Talbot, H. M., Taylor, K. W. R., Tarozo, R., Uchida, M., van Dongen, B. E., van Mooy, B. A. S.,
321 Wang, J., Warren, C., Weijers, J. W. H., Werne, J. P., Woltering, M., Xie, S., Yamamoto, M., Yang,
322 H., Zhang, C. L., Zhang, Y., Zhao, M.. Sinninghe Damsté, J. S., 2013b. An interlaboratory study of
323 TEX_{86} and BIT analysis of sediments, extracts, and standard mixtures. Geochem. Geophys.
324 Geosyst. 14, 5263–5285.
325 Sinninghe Damsté, J.S., Hopmans, E.C., Pancost, R.D., Schouten S., Geenevasen J.A.J., 2000. Newly
326 discovered non-isoprenoid dialkyl diglycerol tetraether lipids in sediments. Journal of the
327 Chemical Society, Chemical Communications, 1683-1684.
328 Sinninghe Damsté, J.S., Hopmans, E.C., Schouten, S., van Duin, A.C.T. and Geenevasen, J.A.J., 2002.
329 Crenarchaeol: The characteristic core glycerol dibiphytanyl glycerol tetraether membrane lipid of
330 cosmopolitan pelagic crenarchaeota. Journal of Lipid Research, 43, 1641-1651.
331 Snyder, L.R., Kirkland, J.J., Glajch, J.L., 1997. Practical HPLC Method Development. John Wiley & Sons,
332 New York, USA, 2nd ed., pp 211.
333 Weber, Y., De Jonge, C., Rijpstra, W.I.C., Hopmans, E.C., Stadnitskaia, A., Schubert, C.J., Lehmann, M.F.,
334 Sinninghe Damsté, J.S., Niemann, H., 2015 Identification and carbon isotope composition of a
335 novel branched GDGT isomer in lake sediments: Evidence for lacustrine brGDGT production?
336 Geochim. Cosmochim. Acta 154, 118-129.

Weijers, J.W.H., Schouten, S., van Den Donker, J.C., Hopmans, E.C., Sinninghe Damsté, J.S., 2007a. Environmental controls on bacterial tetraether membrane lipid distribution in soils. Geochimica et Cosmochimica Acta 71, 703-713.

Yang, H., Lü X., Ding, W., Lei, Y., Dang X., Xie, S., 2015. The 6-methyl branched tetraethers significantly affect the performance of the methylation index (MBT') in soils from an altitudinal transect at Mount Shennongjia. Organic Geochemistry 82, 42-53.

Zech, R., Gao, L., Tarozo, R., Huang, Y., 2012. Branched glycerol dialkyl glycerol tetraethers in Pleistocene loess-paleosol sequences: Three case studies. Organic Geochemistry 53. 38–44.

Zhu C., Yoshinaga M.Y., Peters C.A., Liu X.-L., Elvert M., Hinrichs K-U., 2014. Identification and significance of unsaturated archaeal tetraether lipids in marine sediments. Rapid Communications in Mass Spectrometry 28, 1144–1152.

Figure captions

Figure 1. LC-MS analysis of GDGTs in sediment sample D2 from Drammersfjord, Norway using 2 UHPLC silica column in series. (a) base peak chromatogram ; (b) mass chromatograms of isoprenoid GDGTs used in TEX_{86} with number of cyclopentane rings indicated, the most abundant of the minor isomers is indicated with '; (c) mass chromatograms of branched GDGTs showing the 5- and 6-methylated isomers for the hexa- and pentamethylated brGDGTs, while the tetramethylated brGDGTs are indicated by a *; and (d) enlargements of the area indicated by dashed boxes in (i) the mass chromatogram of *m/z* 1292 detailing the separation between crenarchaeol (cren) and its regioisomer (cren') and (ii) the mass chromatogram of *m/z* 1050 detailing the separation between the 5- and 6-methylhexamethylated branched GDGTs (5 and 6, respectively). All mass chromatograms are at m/z values corresponding to the protonated molecules of the indicated GDGTs.

363

364 **Figure 2.** Cross plots of GDGT-based proxies determined using the CN column or 4 x Si columns vs. 2

365 UHPLC silica columns: (A) $TEX_{86,CN}$ vs. $TEX_{86,\ UHPLC}$; (B) $MBT'_{5Me,4xSi}$ vs. $MBT'_{5Me,UHPLC}$; (C)$CBT_{5Me,\ 4xSi}$ vs.

366 $CBT_{5Me,\ UHPLC;}$ CBT'_{4xSi} vs. CBT'_{UHPLC}. Linear regression equations and correlation coefficients are shown

367 in each plot; 1:1 lines (red dash) are plotted when not obscured by the data trend lines.

368

369 **Table 1:** Chromatographic resolution calculated according to Eq. [1] for critical pairs in the GDGT

370 chromatography for different methods.

Critical pair[1]	**2 x BEH HILIC Si**	**4 x Si**	**CN**	**2 x BEH HILIC amide**[2]
GDGT-1'/GDGT-1	1.37	1.51	0.87	1.08
GDGT-2'/GDGT-2	1.46	1.71	1.14	1.16
GDGT-3'/GDGT-3	1.32	1.28	0.91	0.65
GDGT-4/crenarchaeol	1.06	nd	nd	0.83
cren/cren'	3.71	3.85	2.51	2.04
5-hexaMe-brGDGT/6-hexaMe-brGDGT	1.62	1.33	-[3]	nr[4]
5-pentaMe-brGDGT/6-pentaMe-brGDGT	0.72	0.64	-	nr

371 [1] Critical pairs listed are shown in figure 1 and indicated by their number of rings with or without ‘
372 [2] Becker et al. (2013)
373 [3] resolution below 0.5.
374 [4] Not reported

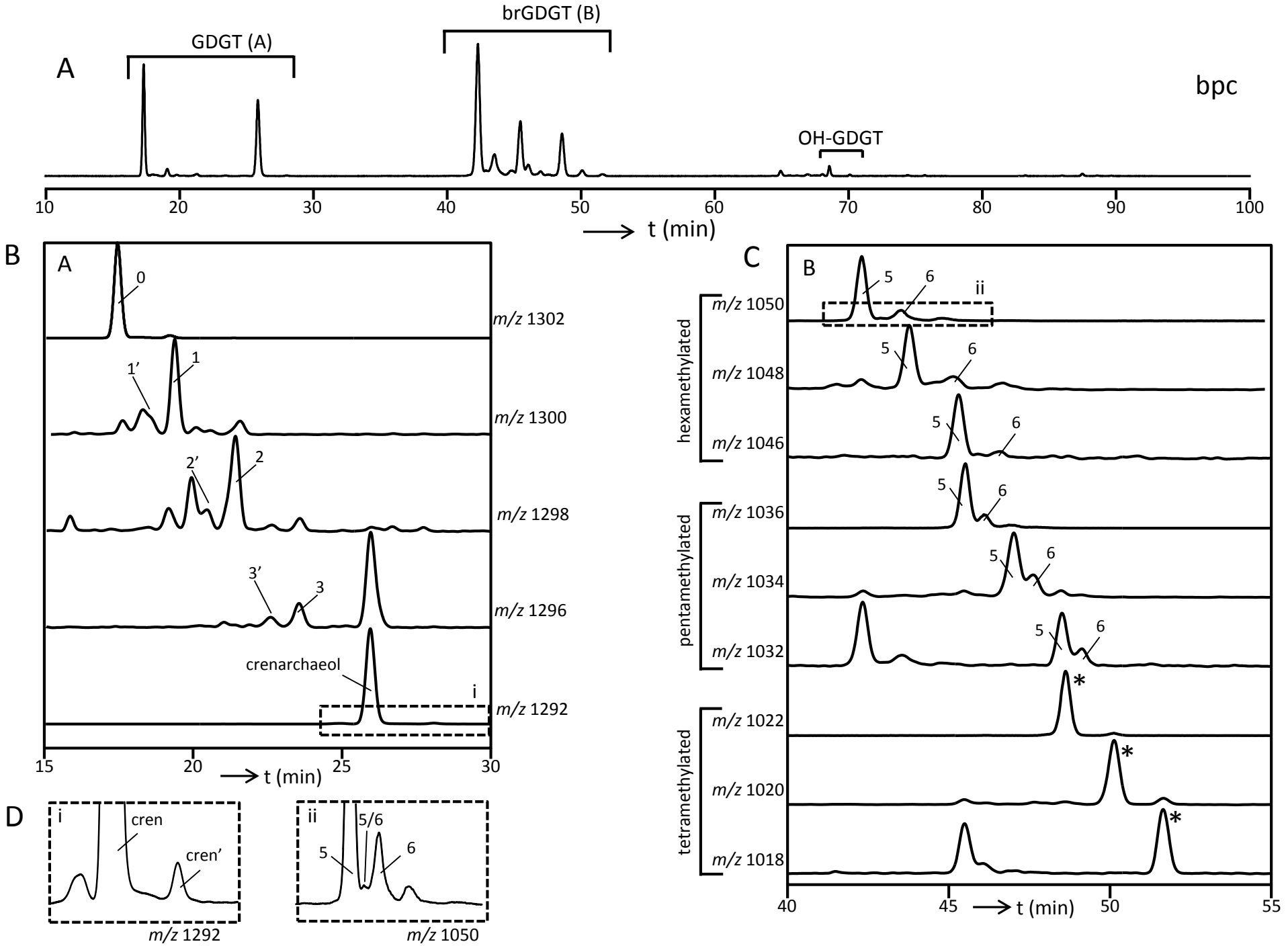
A
GDGT (A)
brGDGT (B)
OH-GDGT
bpc
10
20
30
40
50
60
70
80
90
100
t (min)
B
A
0
m/z 1302
1'
1
m/z 1300
2'
2
m/z 1298
3'
3
m/z 1296
crenarchaeol
i
m/z 1292
15
20
25
30
t (min)
C
B
5
6
ii
m/z 1050
m/z 1048
m/z 1046
hexamethylated
m/z 1036
m/z 1034
m/z 1032
pentamethylated
*
m/z 1022
m/z 1020
m/z 1018
tetramethylated
40
45
50
55
t (min)
D
i
cren
cren'
m/z 1292
ii
5/6
5
6
m/z 1050

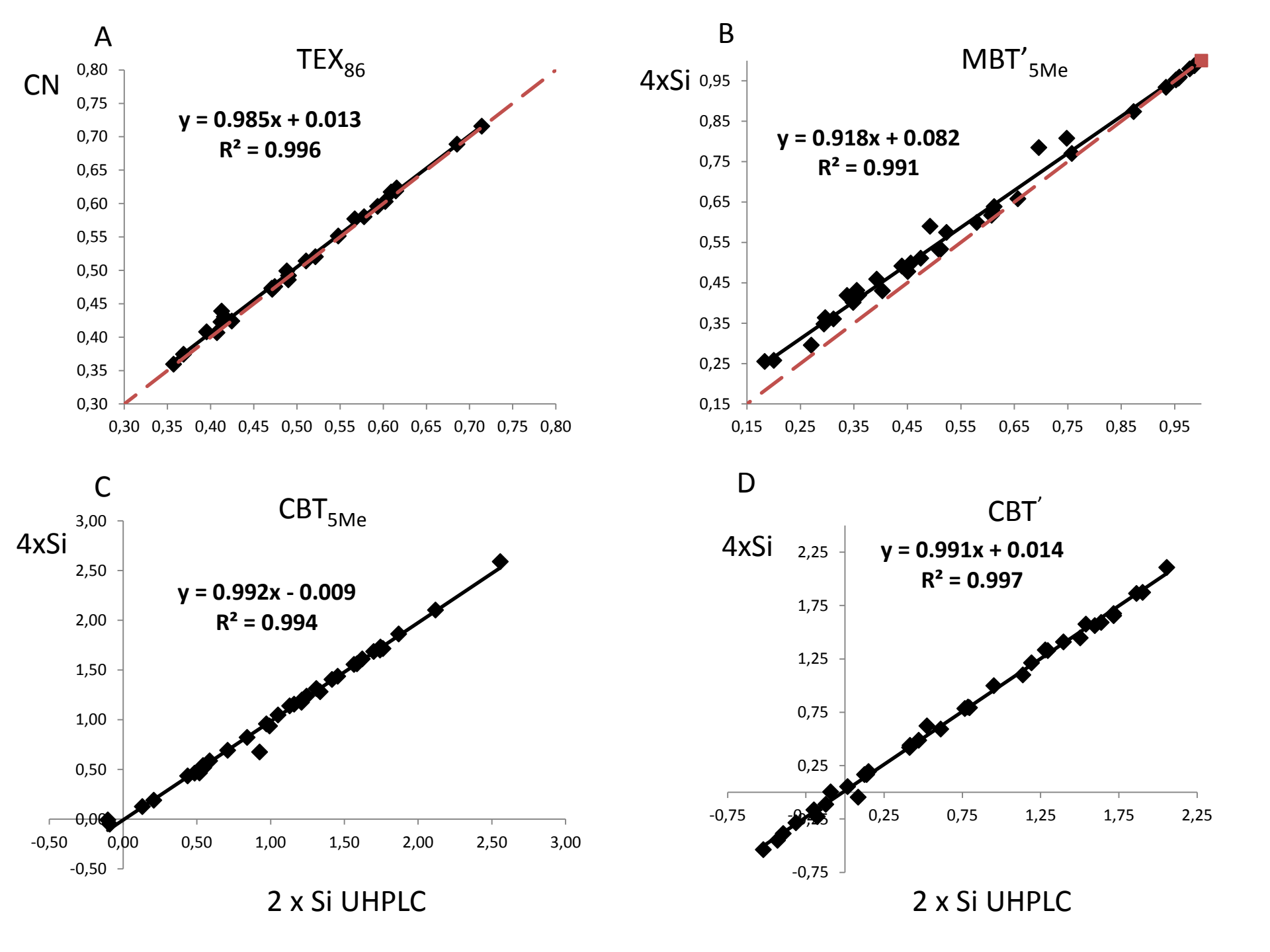
A
TEX86
CN
y = 0.985x + 0.013
R² = 0.996
0,80
0,75
0,70
0,65
0,60
0,55
0,50
0,45
0,40
0,35
0,30
0,30 0,35 0,40 0,45 0,50 0,55 0,60 0,65 0,70 0,75 0,80
B
MBT'5Me
4xSi
y = 0.918x + 0.082
R² = 0.991
0,95
0,85
0,75
0,65
0,55
0,45
0,35
0,25
0,15
0,15 0,25 0,35 0,45 0,55 0,65 0,75 0,85 0,95
C
CBT5Me
4xSi
y = 0.992x - 0.009
R² = 0.994
3,00
2,50
2,00
1,50
1,00
0,50
0,00
-0,50
-0,50 0,00 0,50 1,00 1,50 2,00 2,50 3,00
2 x Si UHPLC
D
CBT'
4xSi
y = 0.991x + 0.014
R² = 0.997
2,25
1,75
1,25
0,75
0,25
-0,75
-0,75 0,25 0,75 1,25 1,75 2,25
2 x Si UHPLC

UHPLC-method-Supplementary Table

Isoprenoid GDGT's

Sample code (Kim et al. 2010)	**TEX86**	
	UHPLC	**CN**
NP-07-13-64	0,41	0,44
GeoB6423-1 0-1	0,55	0,55
GeoB8314-1 0-1	0,49	0,50
GeoB10026-2 0-1	0,71	0,72
GeoB6425-1 0-1	0,58	0,58
GeoB9521-3 0-1	0,59	0,60
GeoB9501-4 0-1	0,57	0,58
GeoB2827-2 0-1	0,61	0,62
GeoB6405-8 0-1	0,42	0,42
GeoB2804-2 0-1	0,47	0,47
GeoB6419-1 0-1	0,51	0,51
GeoB8305-1 0-1	0,49	0,49
GeoB8323-1 0-1	0,42	0,43
GeoB2106-1 0-1	0,62	0,62
GeoB2719-3 0-1	0,36	0,36
GeoB6417-2 0-1	0,47	0,47
GeoB2718-1 0-1	0,40	0,41
IS-S3	0,52	0,52
GeoB2818-1 0-1	0,61	0,62
GeoB10042-2 0-1	0,69	0,69
GeoB6408-3 0-1	0,41	0,42
GeoB1506-1 0-1	0,60	0,60
GeoB6409-2 0-1	0,49	0,49
GeoB2724-7 0-1	0,37	0,37
GeoB6416-2 0-1	0,47	0,48
GeoB6413-4 0-1	0,41	0,41

Branched GDGT's

Sample code (De Jonge et al 2014)	MBT		CBT		MBT'5ME		CBT'	
	UHPLC	4XSi	UHPLC	4XSi	UHPLC	4XSi	UHPLC	4XSi
BRA14 0-9	0,93	0,93	2,56	2,59	0,93	0,93	1,64	1,59
CO9 0-10	0,99	0,99	2,12	2,10	0,99	0,99	2,06	2,11
GB 291	0,96	0,96	0,59	0,58	0,96	0,96	0,79	0,80
Geig1	0,52	0,57	0,99	0,94	0,52	0,57	0,52	0,62
PE10 0-10	0,96	0,96	1,87	1,86	0,96	0,96	1,86	1,86
EC06 pol	0,95	0,95	1,21	1,20	0,95	0,95	1,40	1,41
CND14 103	0,61	0,62	1,57	1,55	0,61	0,62	1,60	1,56
feb-09	0,47	0,51	0,55	0,52	0,47	0,51	0,14	0,17
Wood	0,76	0,77	1,76	1,72	0,76	0,77	1,72	1,67
ZR 404	0,98	0,98	1,74	1,70	0,98	0,98	1,90	1,87
GL I Greenland	0,39	0,46	1,24	1,24	0,39	0,46	0,61	0,59
ZA12 69	0,87	0,87	1,74	1,73	0,87	0,87	1,28	1,34
USA CO3	0,51	0,53	1,13	1,14	0,51	0,53	0,47	0,49
USA CO1	0,29	0,35	1,34	1,28	0,29	0,35	0,41	0,42
NL_MA (2)	0,48	0,57	-0,10	-0,01	0,49	0,59	-0,52	-0,54
USA IT1	0,51	0,53	0,97	0,96	0,51	0,53	0,76	0,79
USA IE4	0,65	0,66	0,21	0,19	0,66	0,66	0,12	0,17
USA MP2	0,31	0,36	1,70	1,69	0,31	0,36	1,72	1,66
USA SR2	0,34	0,41	0,52	0,46	0,34	0,42	-0,43	-0,45
MP6 Svalbard	0,18	0,25	0,44	0,43	0,18	0,25	-0,12	-0,11
MP2 Svalbard	0,28	0,36	0,48	0,46	0,30	0,36	-0,31	-0,29
USA SR3	0,27	0,30	1,16	1,16	0,27	0,30	0,02	0,05
NA1 Svalbard	0,20	0,25	0,54	0,54	0,20	0,26	-0,20	-0,16
USA RT1	0,74	0,80	-0,09	-0,05	0,75	0,81	-0,18	-0,23
USA CF1	0,61	0,63	1,21	1,20	0,61	0,63	1,50	1,45
TESO 5 2-7 F3	0,45	0,49	1,05	1,05	0,46	0,50	0,95	1,00
TESO 10 OC F3	0,35	0,43	0,84	0,82	0,36	0,43	-0,09	0,00
TESO 31 OC F3	0,69	0,78	0,13	0,12	0,70	0,78	-0,40	-0,39
TESO 18 OC F3	0,44	0,49	1,45	1,44	0,44	0,49	1,14	1,10
TESO 3 0-10 F3	0,40	0,43	1,31	1,31	0,40	0,43	1,30	1,33
TESO 24 OC F3	0,45	0,47	0,93	0,68	0,45	0,48	0,08	-0,04
CHA 34 - MG 3769	0,35	0,40	1,58	1,56	0,35	0,40	1,19	1,21
CHA 31 - MG 3676	0,36	0,42	1,42	1,40	0,36	0,42	0,80	0,79
I14 100	0,61	0,64	1,21	1,17	0,61	0,64	0,42	0,44
CHA 39 - MG 3140	0,58	0,60	1,62	1,61	0,58	0,60	1,54	1,58
CHA 16 - MG 2350	0,52	0,55	0,71	0,69	0,52	0,56	0,15	0,20